COMPDYN 2011
3rd ECCOMAS Thematic Conference on
Computational Methods in Structural Dynamics and Earthquake Engineering
M. Papadrakakis, M. Fragiadakis, V. Plevris (eds.)
Corfu, Greece, 25-28 May 2011

ON THE POTENTIAL OF LOCAL RESONATORS TO OBTAIN LOW-FREQUENCY BAND GAPS IN PERIODIC LIGHTWEIGHT STRUCTURES

Claus C. Claeys, Paul Sas and Wim Desmet

Department of Mechanical Engineering,
Katholieke Universiteit Leuven
Celestijnenlaan 300B, B-3001 Heverlee (Leuven), Belgium
e-mail: claus.claeys@mech.kuleuven.be

Keywords: local resonators, band gap, vibro-acoustic insulation, lightweight structures

Abstract. *Periodic structures, such as honeycomb core panels, combine excellent mechanical properties with a low mass, making them attractive for application in transport and machine design. However, the high stiffness to mass ratio of these lightweight panels may result in unsatisfactory dynamic behavior in that it may impair the panels' ability to reduce noise and vibration levels. Their noise and vibration properties can be improved by the application of band gaps, i.e. zones with no free wave propagation. As indicated by Brillouin, periodic structures can exhibit band gap behavior, which in the case of sandwich panels could lead to frequency zones of reduced sound radiation or improved sound transmission loss. Band gaps are commonly the result of interference of traveling waves on the unit cell level, which implies that the lower limit of band gap zones is set by the length scale of the unit cell. However, band gaps can also be obtained by the addition of local resonators. These local resonance band gaps can be freely tuned in a low-frequency zone, independent of the unit cell scale length, making them an appealing engineering tool to improve the dynamic behavior of periodic lightweight structures. By means of numerical models the potential of local resonance band gaps for lightweight periodic panels is shown and compared with interference based band gaps.*

1 INTRODUCTION

For the improvement of vibro-acoustic attenuation a variety of methods exists. Conventional methods rely on the acoustic mass law or the addition of an absorptive layer. The first method results in heavy materials. The second method leads to thick materials, since to be efficient, the thickness of the absorptive layer should be in the same order of magnitude as the acoustic wave length. Often both methods are unsatisfactory to improve the low-frequency vibro-acoustic response of lightweight applications.

The noise and vibration properties of periodic structures can be improved by the application of band gaps, i.e. zones with no free wave propagation. As indicated by Brillouin [1], periodic structures can exhibit such band gap behavior. These gaps result in frequency zones of attenuated structural response. The question arises whether the band gap behavior can be exploited to produce sandwich panels with reduced sound radiation or improved sound transmission loss.

The understanding of periodicity in material crystals and the resulting energy band gaps has led to a high number of applications in solid state physics, such as 'photonic crystals'. Recently quite some research has been performed to transfer these concepts to elastodynamics. Often these band gaps are obtained by incorporating a periodic distribution of wave scatters distributed in a matrix material. These 'phononic crystals' show attenuation of elastic waves in certain frequency bands, although often outside the audible frequency range. Recently, band gaps are actively pursued in order to obtain better structural dynamic behavior in periodic engineering systems such as truss core structures, stiffened plates and cylindrical shells [2, 3, 4].

In solid state physics, there are two theoretical approaches to the understanding of band gaps [5]. The first approach is based on Bragg scattering: zones with destructive interference between reflected and transmitted waves and hence high reflection and low transmission [6]. A second approach utilizes the tight-binding approach, starting from individual atoms/molecules, consisting of well-defined discrete electronic states. Where the first approach is dependent on the wavelength and relies strongly on periodicity, the second approach has as key element the discrete electronic states in individual atoms/molecules and the existence of local modes or local resonances.

The main physical principle behind the band gaps in aforementioned applications is the interference of traveling waves on the unit cell level. This implies that the frequency zone of the band gap is linked to the length scale of the unit cell which is a major drawback to obtain low frequency band gaps. Examples of applications based on the second approach are more scarce, although this method is equally well applicable to elastodynamics problems. In recent literature, examples of this second approach show a huge potential for vibro-acoustic problems [7, 8]. The decoupling of band gap frequency and unit cell length scale opens up the possibility of low frequency vibro-acoustic attenuation, beating the mass law.

This paper compares both methods of band gap creation with respect to vibro-acoustic attenuation. Mainly two characteristics are investigated: strength of vibro-acoustic attenuation and ease of manipulation of the band gap frequencies. Since band gaps show up as zones with no free wave propagation in infinite structures, only infinite structures are investigated. The first section elaborates on the modeling techniques used. The second section provides a one

dimensional example to illustrates the difference in attenuation factors. In a third section, a two dimensional example is used to compare band gap frequencies.

2 MODEL OF PERIODIC STRUCTURES

2.1 Bloch's theorem

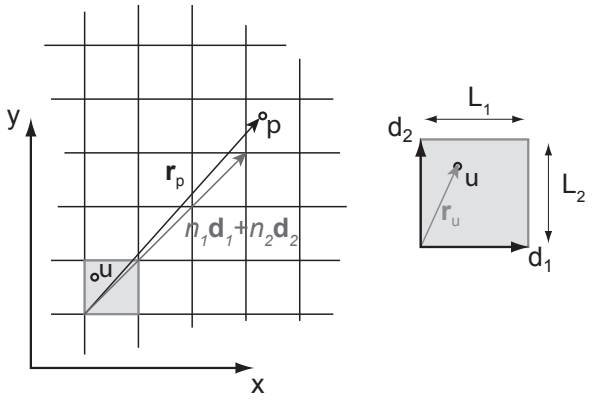

Figure 1: Schematic presentation of an infinite periodic structure (left). The shaded rectangle (right) represents a unit cell of the structure. Each point *p* in the structure can be expressed with respect to a corresponding point *u* in the unit cell.

Figure 1 represents a schematic view of a two-dimensional periodic structure. The structure is built as a repetition of the unit cell in two directions ($\mathbf{d}_1$ and $\mathbf{d}_2$), with $\mathbf{d}_1$ and $\mathbf{d}_2$ basis-vectors of the unit cell with length L_1 and L_2, respectively. Since the structure is periodic, each point *p* in the structure can be expressed with respect to a corresponding point *u* in the unit cell, translated n_1 cells along $\mathbf{d}_1$ and n_2 times along $\mathbf{d}_2$ (Fig. 1):

$$\mathbf{r}_p = \mathbf{r}_u + n_1\mathbf{d}_1 + n_2\mathbf{d}_2 \tag{1}$$

The theorem of Bloch (eq. 4) states that the response of a two-dimensional periodic system can be expressed in terms of the response of a reference unit cell, and an exponential term defining amplitude and phase change as the wave propagates from one cell to the next [1, 9]. The proportionate change in wave amplitude occurring when transitioning from one cell to the next, is independent of the cell location within the periodic system.

$$u(\mathbf{r}_p, \omega) = u_{ref}[\mathbf{r}_u, \omega].e^{\mathbf{k}.(n_1\mathbf{d}_1+n_2\mathbf{d}_2)} \tag{2}$$

The amplitude and phase change is determined by the wave vector $\mathbf{k}$, which is a general term expressing the amplitude decay and phase change of a wave per meter. In practice the wave vectors are expressed in terms of the length of the unit cell:

$$\boldsymbol{\mu} = \mathbf{k}.\mathbf{d} \tag{3}$$

The propagation vector $\boldsymbol{\mu}$ (eq. 3) expresses the complex phase shift when moving across a cell in the $\mathbf{d}_1$ $\mathbf{d}_2$-direction. With this notation the Bloch theorem is rewritten as:

$$u(\mathbf{r}_p, \omega) = u_{ref}[\mathbf{r}_u, \omega].e^{\boldsymbol{\mu}.\mathbf{n}} \tag{4}$$

Where $\mathbf{n}$ is a vector indicating the amount of cells moved in the $\mathbf{d}_1$- and $\mathbf{d}_2$-direction with respect to the unit cell.

2.2 Modelling the unit cell

Since the response of the entire structure is characterized by the response of the unit cell, a model of the unit cell suffices to investigate the wave propagation in the entire structure.

The finite element approach is chosen to model the unit cell [10, 11]. The equation of motion for harmonic motion is written in the usual matrix form:

$$(\mathbf{K} - \omega^2\mathbf{M})\mathbf{q} = \mathbf{f} \tag{5}$$

with $\mathbf{K}$ the stiffness matrix, $\mathbf{M}$ the mass matrix, $\mathbf{q}$ the generalized displacements, $\mathbf{f}$ the generalized forces and ω the angular frequency.

The equation of motion (Eq. 5) can be reduced by taking the boundary condition of the unit cell into account. The Bloch theorem states that the displacements and the forces are scaled with a factor e^{μ_1} and e^{μ_2} when moving from one cell to the next in the $\mathbf{d}_1$- resp. $\mathbf{d}_2$-direction. Demanding compatible displacements and force balance at the boundaries of the unit cell, a reduction matrix $\boldsymbol{R}$ in terms of the wave vector $\boldsymbol{\mu}$ can be derived [12].

$$\begin{aligned}(\mathbf{K} - \omega^2\mathbf{M})\mathbf{q} &= \mathbf{f} \\ \mathbf{R}^{*^T}(\mathbf{K} - \omega^2\mathbf{M})\mathbf{R}\mathbf{q}^{(red)} &= \mathbf{R}^{*^T}\mathbf{f}\end{aligned} \tag{6}$$

Under the assumption of no internal forces, the reduced force vector ($\mathbf{R}^{*^T}\mathbf{f}$) equals the zero vector and the equation of motion (eq. 5) reduces to an eigenvalue problem (eq. 7) in terms of the reduced stiffness and mass matrices $\mathbf{K}^{(red)} = \mathbf{R}^{*^T}\mathbf{K}\mathbf{R}$ and $\mathbf{M}^{(red)} = \mathbf{R}^{*^T}\mathbf{M}\mathbf{R}$.

$$(\mathbf{K}^{(red)} - \omega^2\mathbf{M}^{(red)})\mathbf{q}^{(red)} = \mathbf{0} \tag{7}$$

In this paper two approaches are used to solve this eigenvalue problem.

Direct approach In one-dimensional problems only propagation in one direction exists: the propagation vector $\boldsymbol{\mu}$ reduces to a complex scalar μ. For each frequency the eigenvalue problem can be rewritten in a polynomial form in terms of e^{μ} which can be solved for [13]. Stop bands are frequency zones where free wave propagation is inhibited and thus the propagation constant has a real part. Inspection of the propagation constant results therefore in the identification of stop bands.

Inverse approach Assuming free wave propagation, the propagation vector is strictly imaginary $\boldsymbol{\mu} = i\boldsymbol{\epsilon}$. Solving Eq. 7 for the frequency ω as a function of imaginary propagation vector $\boldsymbol{\epsilon}$, the frequencies of free wave propagation are found. In the case of imaginary propagation constants, the matrix $(\mathbf{K}^{(red)} - \omega^2\mathbf{M}^{(red)})$ is Hermitian and the solutions for ω are always real [12].

Considering the advantage of obtaining complex propagation constants, the first method will be applied to gain insight in the difference in attenuation factors between interference based and local resonance based band gaps. The second method will be used to investigate the manipulation of band gap frequencies for structures with two-dimensional periodicity.

2.3 Irreducible Brillouin contour

To obtain the pass and stop bands with the inverse approach, eq. 7 needs to be solved for every possible combination of purely imaginary propagation constants $\mu_1 = i\epsilon_1$ and $\mu_2 = i\epsilon_2$. The solved frequencies make up a surface in the wave domain (ϵ_1, ϵ_2), the so called dispersion surface $\omega = f(\epsilon_1, \epsilon_2)$. This dispersion surface yields the frequencies for which wave propagation without attenuation is possible. The frequencies which are not a solution of the eigenvalue problem, are frequencies where only attenuated wave propagation is possible and thus these frequencies belong to stop bands.

Since the analyzed structure is periodic, also the dispersion surface will be periodic and hence not the entire wave domain must be investigated. A periodic zone in the wave domain is called a Brillouin zone, and only the first Brillouin zone needs to be examined [1, 6]. Exploiting the symmetry of the unit cell, the first Brillouin zone can be further reduced to an irreducible Brillouin zone which is the smallest zone in the wave space that comprehends all information [2, 14].

A further reduction in computational cost can be achieved by limiting the variation of the wave vector along the contour of the irreducible Brillouin zone. The maxima and minima of each dispersion surface can be found on this boundary. The resulting dispersion curves contain sufficient information for the calculation of band gaps. Although this procedure is widely accepted in literature, according to the authors, no rigorous proof of this is available, but also no counterexamples can be found.

In this paper, the unit cell will be limited to a symmetric rectangular unit cell. As a result in the (ϵ_1, ϵ_2) domain only the contour with corner points $(0, 0), (0, \pi), (\pi, \pi), (0, 0)$ needs to be investigated [2].

3 ATTENUATION FACTOR

To drastically improve the vibro-acoustic behavior, a strong vibro-acoustic attenuation is required. The propagation vector $\boldsymbol{\mu}$ is a measure of vibro-acoustic attenuation: a larger real part, yields stronger attenuation. To compare attenuation factors for both interference and local resonance band gaps, the direct approach of solving eq. 5 is followed.

An infinite Euler-Bernoulli beam serves as a test case: this example is easy to grasp while computationally non demanding. Periodicity is introduced by the addition of a point mass or a spring-mass system. Table 1 summarizes the material characteristics and cross section dimensions of the infinite beam.

Name	Symbol	Value
Young's modulus	E	210 GPa
Density	ρ	7800 $\frac{kg}{m^3}$
Poisson's ratio	ν	0.3
Cross sectional area	A	$1 * 10^{-4} m^2$
Second moment of inertia (bending)	I	$8.33 * 10^{-10} m^4$

Table 1: Material characteristics and dimensions of the infinite beam used in the examples.

3.1 Interference band gap

Interference results from the combination of reflected and transmitted waves. A point mass without rotational inertia is added repeatedly every distance L to the infinite beam to introduce scatterers for reflection. Figure 2 shows the unit cell of the infinite beam. The added mass is 20% of the mass of the unit cell.

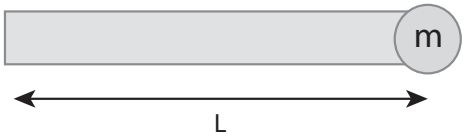

Figure 2: Unit cell of an infinite Euler-Bernoulli beam with a periodic point mass.

Since the band gap is due to interference, the frequency of the band gap is linked to standing wave behavior. The first standing waves will occur for a frequency where the unit cell length (L) equals half a structural wavelength. This condition is mathematically equivalent to claiming that the phase shift across the unit cell ϵ equals π. For an infinite Euler-Bernoulli beam, this frequency for bending equals to:

$$f_{\frac{\lambda}{2}} = \frac{\pi}{2L^2}\sqrt{\frac{EI}{\rho A}}. \tag{8}$$

This frequency $f_{\frac{\lambda}{2}}$ is used to make the frequency in the results dimensionless and independent of the periodicity length.

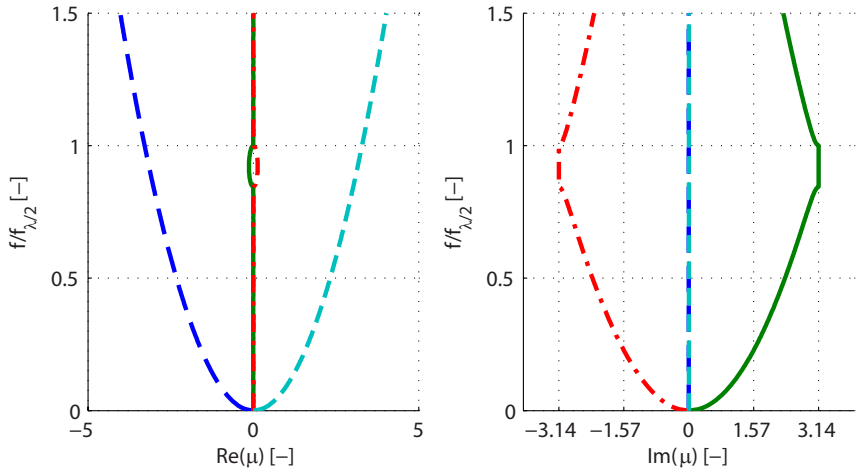

Figure 3: Dispersion curves for an infinite Euler-Bernoulli beam with a periodic point mass. The frequency zone without strictly imaginary wave propagation constant μ indicates a band gap.

Figure 3 shows the calculated propagation constants for a frequency range 0 to $1.5 f_{\frac{\lambda}{2}}$. The solutions for both the right and left running waves are shown. Two different wave types are found. The first wave type (dashed lines) has a purely real wavenumber, expressing a damped exponential decay. The second wave type (full and dash-dotted line) starts as a free propagating

wave with increasing phase shift for increasing frequency. This trend stops as the phase shift ϵ across the unit cell becomes π (dimensionless frequency 0.85). Between dimensionless frequency 0.85 and 1 the imaginary part of the propagation constant μ remains constant and the real part differs from zero. In this frequency zone, no free wave propagation is possible and a band gap is found. For higher frequencies the wave transitions again to a free propagating wave.

3.2 Local resonance band gap

The existence of a local resonance in the unit cell can also lead to a band gap. A periodic repetition of a spring-mass system is added to the infinite Euler Bernoulli beam to simulate this behavior. Figure 4 shows the unit cell. The added mass is 20% of the mass of the unit cell, the stiffness is chosen such that the resonance of the spring-mass system equals $0.5 f_{\frac{\lambda}{2}}$.

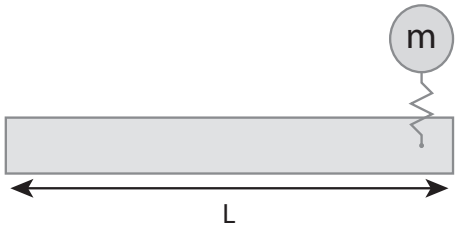

Figure 4: Unit cell of an infinite Euler-Bernoulli beam with a spring-mass periodically attached.

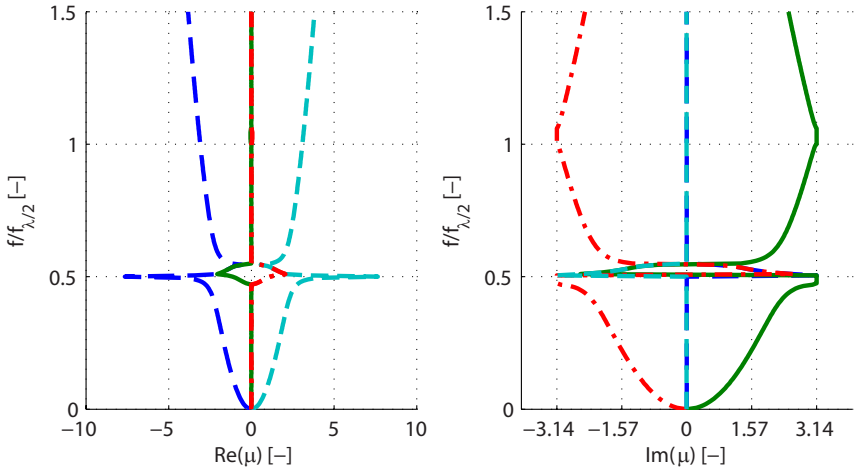

Figure 5: Dispersion curves for an infinite Euler-Bernoulli beam with a periodic spring-mass system. The resonance frequency of the spring-mass system is $0.5 f_{\frac{\lambda}{2}}$. The frequency zone without strictly imaginary wave propagation constant μ indicates a band gap.

The propagation constants for a frequency range 0 to $1.5 f_{\frac{\lambda}{2}}$ are shown in Fig. 5. For frequencies lower than the resonance frequency, the system is very similar to the beam with periodic masses: a free propagating wave (full and dash-dotted line) and a damped wave (dashed lines) are found. In the zone close to the resonance frequency the behavior changes drastically: both wave types have complex propagating constants and a band gap opens up from dimensionless frequency 0.47 to 0.55.
The local resonance band gap is smaller than the interference band gap (Fig.3), but shows very

strong attenuation. For higher frequencies the wave types correspond again with the previous example.

It can be noticed that from dimensionless frequency 1 up to 1.065 a second band gaps opens up, although this band gap has a very low attenuation. This band gap is linked to standing wave behavior and can be explained as scattering due to the impedance of the resonator.

3.3 Comparison

For the same mass addition, the local resonance band gap shows a stronger attenuation, while the interference band gap opens up a larger band gap. The position of the band gap due to interference is linked to the standing wave behavior of the unit cell, whereas for the local resonance the band gap frequencies depend on the resonance frequency of the mass-spring system. The manipulation of band gap frequencies will be investigated in more detail in the next section.

4 BAND GAP FREQUENCIES

To improve vibro-acoustic behavior, it is crucial to be able to control the band gap frequencies. Attenuation in a certain frequency region often suffices to improve the vibro-acoustic behavior of a system drastically.

An infinite steel plate serves as a test case. Periodicity is again introduced by the addition of a point mass or a spring-mass system. Table 2 summarizes the material characteristics and dimensions.

Name	Symbol	Value
Young's modulus	E	210 GPa
Density	ρ	7800 $\frac{kg}{m^3}$
Poisson's ratio	ν	0.3
Thickness	t	$1mm$

Table 2: Material characteristics and dimensions of the infinite plate used in the examples.

Only the dispersion curves linked to out-of-plate motion of the plate will be examined. The in-plane modes of the plate are decoupled from the out-of-plane modes for flat plates and can be omitted from a vibro-acoustic point of view.

4.1 Interference band gap

To investigate interference band gaps, a point mass without rotational inertia is added periodically in two dimensions. The length of repetition in x and y direction is the same, so that the unit cell (Fig. 6) is symmetrical and square. The mass of the point mass is 20% of the mass of the unit cell.

The interference band gap will be linked to the standing wave behavior of the plate, however, now standing waves in different directions are possible. The first standing wave in y direction occurs when the wave length in y direction equals double the length of the unit cell (L). For the

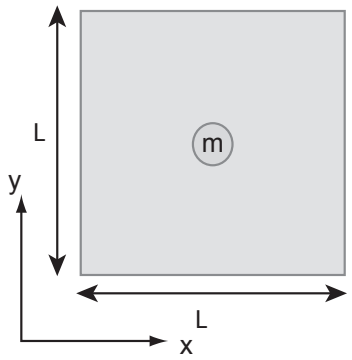

Figure 6: Square unit cell of an infinite plate with a periodic point mass.

x direction the same frequency is found due to symmetry. The first standing wave in diagonal direction occurs when the projected wavelength in both x and y direction equal double the unit cell length, hence when the diagonal wavelength equals $\sqrt{2}L$. These conditions are mathematically equivalent to claiming that the phase shift across the unit cell (ϵ_x, ϵ_y) is equal to $(0, \pi)$ for a wave in y direction and equal to (π, π) for the diagonal wave. It is worth pointing out that these are two of the three corner points of the irreducible Brillouin contour.

For an infinite plate with plane stress assumption the relationship between frequency and wavelength for bending waves is given by:

$$f = \frac{2\pi}{\lambda^2}\sqrt{\frac{t^2 E}{12(1-\nu^2)\rho}}. \tag{9}$$

The frequency for which the wavelength λ equals two times the unit cell length is used to make the frequency in the results dimensionless. Hence for the first standing wave in y direction the dimensionless frequency will by 1, for the first diagonal standing wave the dimensionless frequency will be 2.

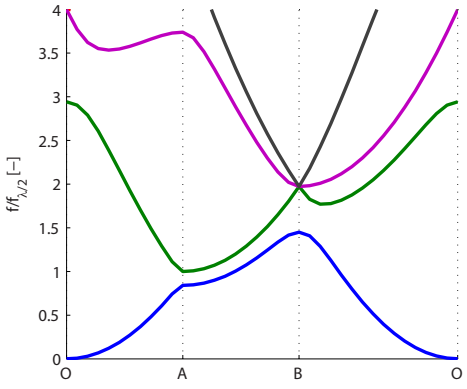

Figure 7: Dispersion curves for an infinite plate with a point mass repeated periodically in two dimensions. The dispersion curves are calculated along the contour of the irreducible Brillouin Contour: O,A,B,O $\mapsto (0,0), (0,\pi), (\pi,\pi), (0,0)$. The added mass is 20% of the unit cell mass.

Figure 7 shows the dispersion curves obtained with the inverse approach. For each frequency there is a corresponding point in the wave domain, and thus direction, for which free

wave propagation is possible. Point A corresponds with propagation constants $(0, \pi)$ and a partial band gap from dimensionless frequency 0.84 to 1 is noticeable. For point B, corresponding with propagation constants (π, π) a partial band gap from dimensionless frequency 1.45 to 2 is found. Interference causes band gaps for waves in a certain direction in the frequency region corresponding to the standing wave in that direction, but these band gaps are not large enough to create a band gap across the entire wave domain.

Figure 8 shows the dispersion curves for an added periodic point mass of 80% of the unit cell. The partial band gap clearly comprises a broader frequency range and the partial band gaps are large enough to result in a complete band gap of $0.07 f_{\frac{\lambda}{2}}$.

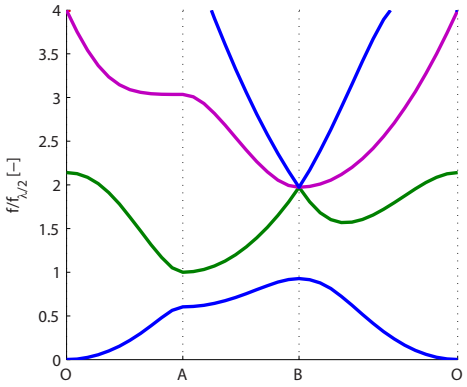

Figure 8: Dispersion curves for an infinite plate with a point mass repeated periodically in two dimensions. The dispersion curves are calculated along the contour of the irreducible Brillouin Contour. The added mass is 80% of the unit cell mass.

4.2 Local resonance band gap

Local resonance band gaps are achieved by the addition of a mass-spring system in the same manner as the point mass in the previous example. Figure 9 shows the unit cell. The mass is 20% of the mass of the unit cell, the stiffness is chosen so that the resonance of the unit cell is at a dimensioless frequency of 0.5.

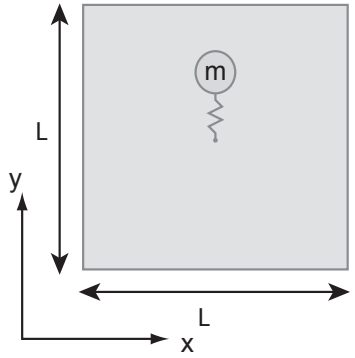

Figure 9: Unit cell of an infinite plate with a spring-mass system periodically attached.

The dispersion diagram (Fig. 10) shows a band gap from a dimensionless frequency of 0.48 up to 0.54. In a frequency region around the resonance frequency of the spring-mass

system, no free wave propagation is possible. The original dispersion curve is pulled down to frequencies below the resonance of the spring-mass system. Above the resonance frequency a new dispersion curve appears. The pulled down dispersion curve relates to in phase movement of plate and resonator; the new dispersion curve contains modes where resonator and plate move out-of-phase.

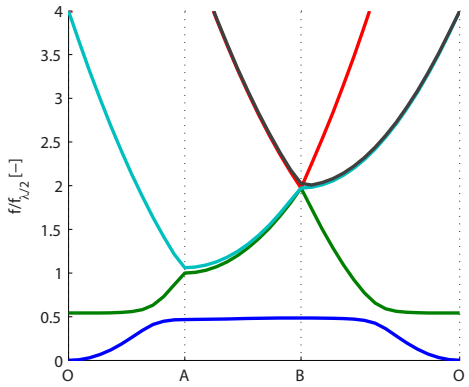

Figure 10: Dispersion curves for an infinite plate with a spring-mass system added periodically in two dimensions. The dispersion curves are calculated along the contour of the irreducible Brillouin Contour: O,A,B,O $\mapsto$ $(0,0),(0,\pi),(\pi,\pi),(0,0)$. The added mass is 20% of the unit cell mass. The resonance frequency of the spring-system is $0.5 f_{\frac{\lambda}{2}}$.

Figure 11 shows the link between band gap width and added mass of the local resonator. The stiffness of spring-mass system is changed in function of the mass addition so that the dimensionless resonance frequency is kept at 0.5. Increasing the mass of the local resonator leads to a larger band gap. Although the lower limit of the band gap is pushed down a little, the higher limit of the band gap is affected the most. This agrees with the statement that the lower limit of the band gap is strongly linked to the local resonator resonance, while the upper limit is more influenced by the interaction of the resonator and the plate [15].

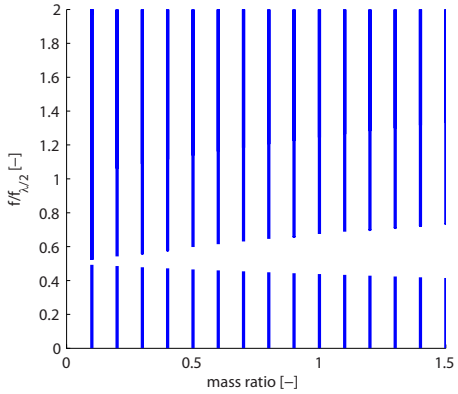

Figure 11: Relationship between frequencies of free wave propagation for an infinite plate with a spring-mass system added periodically in two dimensions and the mass the of spring-mass system. The spring stiffness is adjusted as function of the added mass to keep the resonance frequency fixed at a $0.5 f_{\frac{\lambda}{2}}$.

Figure 12 shows the link between band gap and resonance frequency of the local resonator. The mass of the local resonator is kept at 20% of the plate mass and the stiffness is changed to

change the resonance frequency. For the different resonance frequencies band gaps are calculated, which are represented as white gaps in Fig. 12. Up to a dimensionless frequency of 1, the resulting band gap is always centered at the resonance frequency of the local resonator. For higher frequencies no band gap is found.

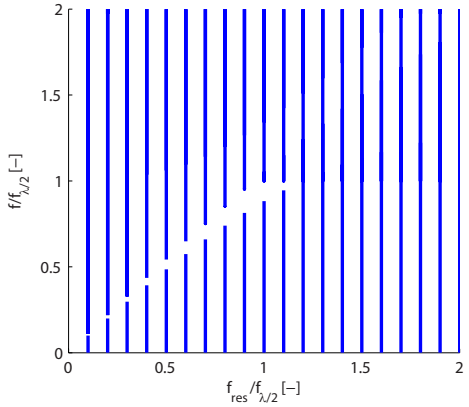

Figure 12: Relationship between frequencies of free wave propagation for an infinite plate with a spring-mass system added periodically in two dimensions and the resonance frequency of spring-mass system. The added mass of the local resonator is 20% of the plate mass.

The upper frequency of the highest band gap obtained is linked to standing wave behavior. Figure 13 shows the dispersion diagram for a spring-mass system with a dimensionless resonance frequency of 1.5. A free propagation wave at a dimensional frequency of 1.5 is found for the point with imaginary propagation constants $(0.72\pi, \pi)$, indicated with a black circle in Fig. 13. This correlates with a standing wave in y-direction and traveling wave in x-direction. In the corresponding wave motion all the spring-mass systems are in nodal points and hence not excited. For frequencies higher than the first standing wave frequency, it will always be possible to have traveling waves for which the mass-spring systems are in nodal positions: the dimensionless frequency of 1 is thus the upper-limit for local resonance band-gaps.

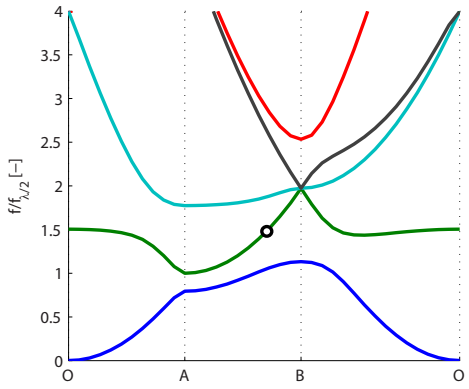

Figure 13: Dispersion curve for an infinite plate with a spring-mass system added periodically in two dimensions. The dispersion curves are calculated along the contour of the irreducible Brillouin Contour: O,A,B,O $\mapsto$ $(0,0), (0,\pi), (\pi,\pi), (0,0)$. The added mass is 20% of the unit cell mass. The resonance frequency of the spring-mass system is $1.5 f_{\frac{\lambda}{2}}$. The black circle indicates the point $(0.72\pi, \pi)$ and dimensionless frequency 1.5.

Figures 14 is the result of a comparable analysis as Fig. 12 but with an added relative

mass of 80%. It is clear that once again no band gaps show up for frequencies higher than a dimensionless frequency 1. Although, this time spring-mass-systems with a dimensionless resonance frequency higher than 1 still result in band gaps. For these resonance frequencies however, the link between resonance frequency and band gap frequency is lost. The resulting band gap is not a purely local resonance band gap: due to the relative large added mass and the resonance frequency in the vicinity of the standing wave frequency, the large impedance of the spring-mass-system at the standing wave frequency will lead to an interference based band gap.

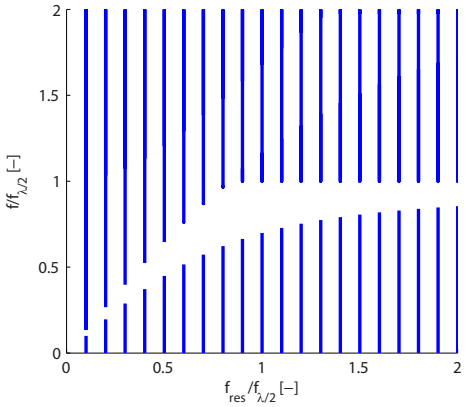

Figure 14: Relationship between frequencies of free wave propagation for an infinite plate with a spring-mass system added periodically in two dimensions and the resonance frequency of spring-mass system. The added mass of the local resonator is 80% of the plate mass.

4.3 Comparison

Although interference is a method of creating band gaps, these band gaps are not guaranteed for two dimensional topologies and can only be formed at frequencies corresponding with standing waves across the unit cell. Local resonance based resonators create a band gap at the frequency of the local resonator although this band gap is only guaranteed for frequencies lower than the first standing wave frequency of the unit cell.
For spring-mass-systems with a high impedance at the standing wave frequency, a combination of local resonance based band gaps and interference band gaps is possible.

5 CONCLUSIONS

This paper shows the potential of band gaps to suppress wave motion in certain frequency ranges. Band gaps can be created due to interference or by the addition of a local resonators in each unit cell.
Interference band gaps are linked to standing wave behavior and are not guaranteed. This explains why, although a lot of panels are periodic, band gaps are not often encountered: either the band gap frequency is too high or a complete band gap is not found.
The periodic introduction of a local resonator introduces a band gap at the resonance frequency of the local resonator. This is the case as long as the resonance frequency of the local resonator is below the first standing wave frequency in the unit cell.
In general the local resonance band gap shows stronger vibro-acoustic attenuation and the frequencies of the band gap are easier to manipulate. In conclusion, local resonance band gaps

seem to have a high potential to improve the vibro-acoustic behavior of periodic lightweight structures in the low-frequency region.

6 ACKNOWLEDGEMENTS

The research of Claus Claeys is funded by a Ph.D. grant of the Institute for the Promotion of Innovation through Science and Technology in Flanders (IWT-Vlaanderen).

REFERENCES

[1] L. Brillouin, *Wave Propagation in Periodic Structures*. Dover, 1946.

[2] A. R. Diaz, A. G. Haddow, L. Ma, Design of band-gap grid structures. *Structural and Multidisciplinary Optimization*, **29**, 418–431, 2005.

[3] S. Lee, N. Vlahopoulis, A.M. Waas, Analysis of wave propagation in a thin composite cylinder with periodic axial and ring stiffeners using periodic structure theory. *Journal of Sound and Vibration*, **329**, 3304–3318, 2010.

[4] S. V. Sorokin, O.A. Ershova, Plane wave propagation and frequency band gaps in periodic plates and cylindrical shells with and without heavy fluid loading. *Journal of Sound and Vibration*, **278**, 501–526, 2004.

[5] P. Sheng, C. Chan, Classic wave localization and spectral gap materials. *International Journal for structural, physical and chemical aspects of crystalline material*, **220**, 757–764, 2005.

[6] C. Kittel, *Introduction to Solid State Physics*. Wiley, 2005.

[7] Z. Liu, X. Zhang, Y. Mao, Y.Y. Zhu, Z. Yang, C.T. Chan, P. Sheng, Locally resonant sonic materials. *Science*, **289**, 1734–1736, 2000.

[8] G. Wang, X. Wen, J. Wen, L. Shao, Y. Liu, Two-dimensional locally resonant phononic crystals with binary structures. *Physical review letters*, **93**, 154302, 2004.

[9] F. Bloch, Über die Quantenmechanik der Elektronen in Kristallgittern. *Zeitschrift fr Physik A Hadrons and Nuclei*, **52**, 555-600, 1929.

[10] J.D. Mead, A general theory of harmonic wave propagation in linear periodic systems with multiple coupling. *Journal of Sound and Vibration*, **27**, 235–260, 1972.

[11] J.D. Mead, Wave Propagation In Continuous Periodic Structures: Research Contributions From Southampton: 1964-1995. *Journal of Sound and Vibration*, **190**, 495–524, 1996.

[12] R. Langley, A note on the force boundary conditions for two-dimensional periodic structures with corner freedoms. *Journal of Sound and Vibration*, **167**, 377–381, 1993.

[13] B.R. Mace, D. Duhamel, M.J. Brennan, L. and Hinke, Finite element prediction of wave motion in structural waveguides. *The Journal of the Acoustical Society of America*, **117**, 2835–2843, 2005.

[14] S.J. Cox, D.C. Dobson, Maximizing band gaps in two-dimensional photonic crystals. *SIAM Journal on Applied Mathematics*, **55**, 2108–2120, 1999.

[15] C. Goffaux, J. Sánchez-Dehesa Two-dimensional phononic crystals studied using a variational method: Application to lattices of locally resonant materials *Physical Review B*, **67**, 144301, 2003.